Desalination and Water Treatment
www.deswater.com
doi: 10.1080/19443994.2015.1077745

57 (2016) 15920–15931
July

Taylor & Francis
Taylor & Francis Group

Removal of phosphate from industrial wastewater using uncalcined MgAl-NO_3 layered double hydroxide: batch study and modeling

Mohamed Khitous[a,b,*], Zineb Salem[a], Djamila Halliche[b]

[a]*Laboratory of Industrial Process and Engineering LSGPI, Faculty of Mechanical and Process Engineering, University of Sciences and Technology, Houari Boumediene, BP 32, El-Allia, Bab Ezzouar 16111, Algiers, Algeria, Tel. +213 21 24 79 19; email: usthbkhitous@yahoo.fr (M. Khitous), Tel. +213 71 17 34 28; email: zsalem141@gmail.com (Z. Salem)*
[b]*Laboratory of Natural Gas Chemistry, Institute of Chemistry, University of Sciences and Technology, Houari Boumediene, BP 32, El-Allia, Bab Ezzouar 16111, Algiers, Algeria, Tel. +213 21 63 66 08; email: dhalliche@yahoo.fr*

Received 27 December 2014; Accepted 24 July 2015

ABSTRACT

In this study, the sorption ability of nitrate containing MgAl layered double hydroxide as an anion-exchanger to remove phosphate from a real effluent was investigated. The LDH material was prepared via coprecipitation method and characterized by X-ray diffraction, SEM, Fourier Transform Infrared, BET surface area, and pH_{zpc}. The effect of physico–chemical key parameters on phosphate removal, such as sorbent dosage, solution pH, initial concentration, and contact time, has been studied in batch mode. The sorption reached equilibrium within 30 min. Furthermore, the sorption mechanism of phosphate onto MgAl-NO_3 LDH is a combination of both anion-exchange and electrostatic attraction. The equilibrium 8 data were tested using Langmuir, Freundlich, and Dubinin–Radushkevich isotherms. The results show that the Langmuir isotherm describes sufficiently the sorption equilibrium, offering a maximum sorption capacity of 64.10 mg/g. Sorption kinetic follows accurately pseudo-second-order reaction. The sorbent reusability shows that regenerated LDH can be reused in subsequent sorption–regeneration cycles with a slight decrease in sorption capacity.

Keywords: Layered double hydroxide; Sorption; Phosphate; Kinetic; Wastewater

1. Introduction

The surface treatment processes applied in the National Company of Appliance Industry in Algeria, generate large volumes of wastewater containing high concentration of phosphate (201 mg P/L). However, excessive phosphate discharged into water bodies like lakes, rivers, and inland seas leads to eutrophication [1]. An abundance of algal blooming in eutrophic water bodies can deplete dissolved oxygen in water, causing the death of fish [2]. On the other hand, some blue-green algae produce compounds that have been implicated in fish and possibly human poisoning [3]. Consequently, the national and international water standard authorities have fixed the tolerance limit for phosphorus effluents from 0.1 to 2.0 mg P/L, and most of them are established at 1.0 mg P/L [4]. Therefore, it is very important to find and develop effective techniques to reduce the concentration of phosphate in effluents to acceptable level before discharging them into water bodies.

*Corresponding author.

Recently, several methods have been used to remove phosphate from wastewaters, including chemical precipitation, adsorption, physical and biological treatments [5]. However, physical methods are usually too expensive or inefficient [6]. Chemical precipitation is considered a very effective method because it is well applied in most wastewater treatment systems. Nevertheless, the expenditure on required chemicals, chemical storage, feeding systems is expensive, and the amount of chemical sludge produced is tremendous [2]. Despite the biological methods being inexpensive, they usually require more complex plant configurations and operating regimes [5]. Compared with these techniques, adsorption is more effective and economical due to its simplicity, stability of treatment, and reduced sludge production [7]. Therefore, various types of sorbents have been used to remove phosphate from aqueous solution, such as calcined alkaline residue [8], calcite [9], iron oxide tailing [10], MIEX resin [11], kaolinite [12], and red seaweed [13].

Layered double hydroxides (LDHs) have attracted wide attention as an effective sorbent [14]. Their general formula is $[M^{2+}_{1-x}M^{3+}_{x}\ (OH)_2]^{x+}\ (A^{n-})x/n\ mH_2O$, where M^{2+} and M^{3+} are the divalent and trivalent cations, respectively. x is the M^{2+}/M^{3+} molar ratio and A^{n-} is the incorporated anion in the interlayer space along with water molecules for charge neutrality and structure stability [15]. LDHs are layered materials with hydroxide sheets, where a net positive charge is developed on the layer due to partial substitution of trivalent by divalent cations [16]. Due to the high charge density of the sheets and the exchangeability of the interlayer anions as well, LDHs have been used in several studies as a sorbent to remove different harmful anions, such as arsenate [17], phosphate [18], fluoride [19], and chromium [20].

The anion-exchange capacity of LDHs is affected by the nature of the interlayer anions initially present and the layer charge density. When the layer charge density is very high, the exchange reaction may become difficult. LDHs have greater affinities for multivalent anions compared with monovalent anions [21,22]. In particular, the favorable lattice stabilization enthalpy associated with CO_3^{2-} results in these anions being difficult to displace in anion-exchange reaction. Therefore, the removal of anions in LDHs by intercalation occurs when the interlayer is intercalated by weak electrostatic interactions with the layers, such as chloride or nitrate.

Several studies have investigated the removal of phosphate by calcined and uncalcined LDHs [19,23–25]. However, until now, studies on the use of nitrate-containing LDHs as anion-exchanger for phosphate removal are scarce [26,27]. Anion-exchange can avoid the change of solution pH. Adjusting the solution pH was unavoidable because it was increasing during the sorption process when calcined LDHs have been used [28]. Furthermore, compared to most of the studies focusing on sorptive properties of LDHs, phosphate sorption mechanisms were partly ignored. Therefore, the objective of this study is to investigate the sorption ability of MgAl-NO_3 LDH to remove phosphate from wastewater that was collected from the surface treatment process in Algeria. The effect of various parameters on phosphate removal, such as sorbent dosage, solution pH, contact time, and initial concentration has been studied in batch mode. The explanation of sorption mechanism has been supported by X-ray diffraction (XRD) and Fourier Transform Infrared (FTIR) spectra. The sorption kinetic and isotherms were also investigated. Finally, sorption–regeneration cycles were evaluated to examine the sorbent reusability.

2. Materials and methods

2.1. Sorbent preparation

MgAl-NO_3 LDH was synthesized by co-precipitation method at constant pH. $Mg(NO_3)_2{\cdot}6H_2O$ and $Al(NO_3)_3{\cdot}9H_2O$ solutions were added drop wise into $NaNO_3$ solution. 50 mL of MgAl precursor solution containing 0.025 mol Mg^{2+} and 0.0125 mol Al^{3+} was added to 50 mL of anion solution containing 0.025 mol NO_3^-. The pH of precipitation was adjusted to 10 by adding NaOH solution at 3.4 M under vigorous stirring. The precipitate formed was aged at 60°C in an oil bath shaker for 24 h, cooled, and filtered. The obtained precipitate was washed repeatedly with distilled water to reach a neutral pH and then dried at 80°C for 24 h. Finally, the resulting solids were ground manually in a mortar and sieved to yield powders of 50–100 μm in diameter.

2.2. Characterization of sorbent

Powder XRD analyses were carried out to identify the LDH phase using an XPERT-PR diffractometer, with CuKα radiation ($\lambda = 1.54060$ Å) at 45 kV and 40 mA. Scanning diffraction angle is set at the speed of 0.06°/s. The BET surface area and average pore diameter were measured from the N_2 adsorption/desorption isotherms at 77 K by using Tri-Star II 3020 V1.03 micromeretics surface area and pore size analyzer. The morphology of LDH sample before and after sorption of phosphate was viewed by scanning electron microscopy using an XL30 ESEM at accelerating voltage of 20 kV.

Elemental chemical analysis was performed using an inductivity coupled plasma emission spectrometer for metal ions to determine the Mg/Al molar ratio of the prepared LDH. 0.04 g of sample was dissolved in solution containing 15 mL of HNO_3 and 5 mL of HCl. FTIR spectra of material before and after sorption were recorded using an Alpha Bruker FTIR spectrometer over the 4,000–400 cm^{-1} wave number range.

The pH at the point of zero charge pH_{zpc} of LDH was determined using NaCl solutions at 0.10 and 0.05 M as inert electrolyte. The initial pH was adjusted from 2 to 13 by adding HNO_3 and NaOH solutions at 0.1 M. The experiments were performed on thermostatic stirrer at 200 rpm and 20°C for 2 h, by contacting 20 mg of LDH sample to 100 mL of each solution. Then, the suspensions were filtered and the final pH was measured. The pH_{zpc} was obtained through the plot of pH_{final} vs. $pH_{initial}$ [29].

2.3. Characterization of wastewater

The wastewater used in this study was collected from the national company of appliance industry situated in Algeria. It was characterized for pH, conductivity, total and volatile suspended solids, COD and various anions, as shown in Table 1. The anions were analyzed using a scalar analyzer.

The results obtained in Table 1 indicate a high phosphate concentration of 201 mg/L along with large concentration of other anions like Cr(VI) (35 mg/L), sulfate (116 mg/L), nitrites (86 mg/L), and chloride (111 mg/L). It appears that the phosphate concentration is much higher than the permissible limit for phosphate discharge in wastewater (10 mg P/L). Therefore, wastewater must be treated to reduce the concentration of phosphate to acceptable levels before discharging it into the environment. The concentrations of Cr(VI) and nitrite are also higher than the admissible limits of 0.1 and 1.0 mg/L, respectively.

Table 1
Characteristics of wastewater

Parameter	Value
pH	7.27
Total suspended solids (mg/L)	214
Volatile suspended solids (mg/L)	28
Conductivity (μS/cm)	1,928
COD (mg/L)	<30
PO_4^{3-} (mg/L)	201.43
SO_4^{2-} (mg/L)	116.78
Cl^- (mg/L)	111.25
NO_3^- (mg/L)	49.12
NO_2^- (mg/L)	86.38
Cr(VI) (mg/L)	35.47
HCO_3^- (mg/L)	301.58

2.4. Sorption and kinetic experiments

The experiments were run at room temperature in 100 mL bottles containing 50 mL of solution with a given dose of sorbent. The solution was stirred for 2 h to allow sufficient time for equilibrium.

The sorption of phosphate was studied as a function of solution pH, sorbent dosage, and initial concentration. During the experiments, the studied parameter was varied while other parameters were kept constant. The effect of solution pH was studied at pH values ranging from 2 to 8 at 100 mg P/L and sorbent dose of 2 g/L. The effect of sorbent dosage at 100 mg P/L and pH 6 was investigated at various sorbent quantities ranging from 0.5 to 5 g/L. The effect of initial concentration was studied at phosphate concentrations ranging from 30 to 200 mg P/L, sorbent dose of 2 g/L, and pH 6.

Stock solution was obtained after decantation and filtration of wastewater. The concentration of phosphate in wastewater is 201 mg P/L. It was diluted with distilled water to obtain other concentrations. The pH of solution was adjusted to the desired value by adding negligible volumes of HCl and NaOH solutions at 0.1 M. The phosphate was analyzed by molybdenum blue UV–visible spectrophotometry method at 800 nm [30]. All assays were carried out in triplicate and only mean values are presented.

The sorption capacity was determined from Eq. (1):

$$q_t = \frac{V(C_0 - C_t)}{m} \tag{1}$$

where C_0 and C_t (mg/L) are the initial concentration and the concentration at time t, respectively. q_t (mg/g) is the amount of phosphate sorbed at time t, m (g) the sorbent mass, and V (L) is the volume of solution.

2.5. Equilibrium sorption measurements and modeling

Sorption isotherm was generated by contacting 0.1 g of sorbent with 50 mL of solution containing from 15 to 200 mg P/L. The solutions were stirred for 2 h at room temperature.

The experimental data were analyzed by different sorption models like Langmuir [31], Freundlich [32], and Dubinin–Radushkevich [33] model. The equations are expressed as:

Langmuir:

$$\frac{C_e}{q_e} = \frac{1}{q_m K} + \frac{C_e}{q_m} \quad (2)$$

Freundlich:

$$q_e = K_F C_e^{1/n} \quad (3)$$

Dubinin–Radushkevich:

$$\ln q_e = \ln q_m - K_{DR}\left[RT\ \ln\left(\frac{1}{C_e}\right)\right]^2 \quad (4)$$

$$\varepsilon = RT \ln\left(\frac{1}{C_e}\right) \quad (5)$$

where C_e (mg/L) is the concentration of phosphate at equilibrium, q_e (mg/g) is the sorption capacity at equilibrium, K (L/mg) is Langmuir constant, q_m (mg/g) is the saturated sorption capacity of sorbent, K_F and n are Freundlich parameters, K_{DR} (mol^2/J^2) is the activity coefficient, ε is the Polanyi potential, R is the universal gas constant (8.314 J/mol K), and T (K) is temperature.

The sorption efficiency was predicted by the dimensionless equilibrium parameter, $R_L = 1/(1 + KC_0)$.
where C_0 (mg/L) and K (L/mg) are the highest initial concentration and Langmuir constant, respectively.

The sorption energy was calculated using Eq. (6):

$$E = \frac{1}{(2K_{DR})^{1/2}} \quad (6)$$

where E (J/mol) is the sorption energy.

3. Results and discussion

3.1. Characterization of sorbent

From Fig. 1, it appears clearly that the XRD pattern of the sample has sharp and symmetric peaks at lower 2θ as (0 0 3) and (0 0 6), which are characteristic of the hydrotalcite-like compounds with a high degree of crystallinity. The pattern is indexed to a hexagonal cell [34]. No other phase is observed in the XRD pattern. The basal reflections 0 0 1 at low angles (11°, 2θ) correspond to the interlayer distance of LDH. The (1 1 0) reflection appears at high angles (61°, 2θ). The lattice parameters are estimated as $c = l \times d_{001}$; $a = 2 \times d_{110}$, as shown in Table 2. The results agree well with those

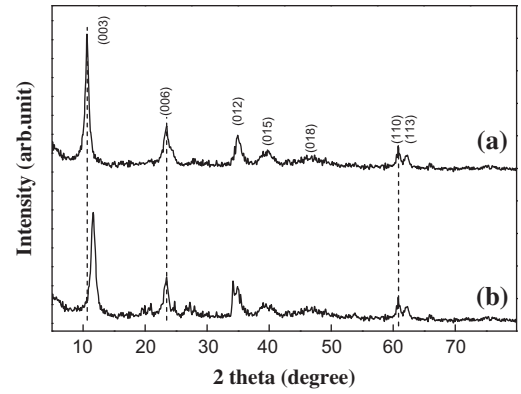

Fig. 1. XRD patterns of MgAl-NO_3 LDH: (a) before and (b) after sorption of phosphate.

reported by Srinivasa et al. [35]. They suggest that a distance of around 8.9 Å is evocative of high interlayer spacing with a thickness of 2–3 atoms. From Fig. 1(b), it can be seen that the characteristic peaks of the LDH structure appear in the XRD pattern of the sample, which indicate that the sorbent remains in its layered structure after anion-exchange with phosphate ions.

However, basal reflection (0 0 3) moves to higher 2θ angle from (d_{003}, 8.37 Å) to (d_{003}, 7.61 Å) after phosphate uptake, indicating that a smaller ion resides in the interlayer region of LDH, because phosphate is a smaller ion than nitrate. The basal reflection (0 0 3) is directly attributed to the interlayer distance of LDH and depends on the size of intercalated anion. In addition, the (1 1 0) reflection of 1.52 Å remains constant with anion-exchange, indicating that the resulting LDH keeps the original lattice parameter (a). Therefore, an anion-exchange mechanism occurs between phosphate and interlayer nitrate.

From Table 2, the resultant Mg/Al molar ratio of the sample was determined to be 1.97, showing a good agreement with the initial value of the starting solutions. Thus, MgAl-NO_3 LDH with Mg/Al molar ratio of 2 was successfully prepared.

The surface area of MgAl-NO_3 LDH is very low (5.70 m^2/g) (Table 2). The result agrees with that reported by Wang et al. [36].

The FTIR spectra of LDH material and its corresponding sample after the uptake of phosphate are shown in Fig. 2. The intense broad band observed at 3,500–3,250 cm^{-1} associated with stretching vibration of O–H bond in the brucite-like layers $Mg(OH)_2$ and $Al(OH)_3$ [37,38]. The band at about 1,643 cm^{-1} can be assigned to the deformation vibration of water molecules in the interlayer domain [39]. The bands at 540–650 cm^{-1} can be due to the vibration of Al–O and Mg–O groups in the layers. The characteristic sharp

Table 2
Characterization of MgAl-NO_3 LDH

Mg/Al molar ratio		BET surface area (m^2/g)	Average pore diameter (nm)	Cell parameters			
Synthesis solution	Obtained sample			d_{003} (Å)	d_{110} (Å)	a (Å)	c (Å)
2	1.97	5.70	10.54	8.369	1.524	3.048	25.11

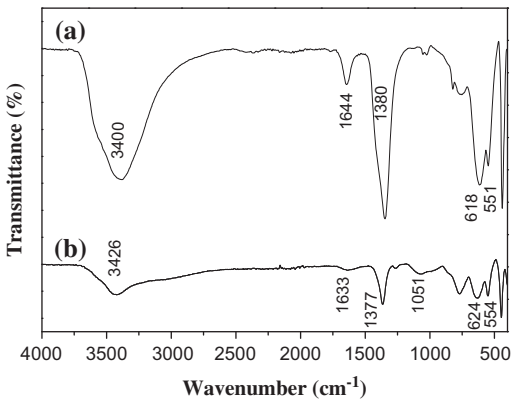

Fig. 2. FTIR spectra of MgAl-NO_3 LDH: (a) before and (b) after sorption of phosphate.

absorption band at about 1,380 cm^{-1} is associated with the antisymetric stretching mode of NO_3^- [40].

From Fig. 2(b), the characteristic bands of the LDH structure were clearly observed in the FTIR spectrum of the LDH sample after sorption of phosphate, but their intensity was significantly reduced compared to that obtained in Fig. 2(a). This indicates that the solid maintains its chemical structure, and anion-exchange reaction occurs between the solid and solution.

As shown in Fig. 2(b), the band observed at 1,377 cm^{-1} becomes weaker and the characteristic band of phosphate appears at 1,051 cm^{-1} [41]. This indicates that the phosphate ions exchange with interlayer nitrate and they are successfully incorporated into the LDH structure. The results agree well with those obtained from XRD pattern. Therefore, anion-exchange mechanism occurs in the removal process of phosphate.

The interlayer nitrate of LDH could be exchanged with phosphate because LDHs have greater affinities for multivalent anions compared with monovalent anions, due to weak electrostatic interactions between the interlayer spacing and brucite sheets [21,22].

The morphology of synthesized LDH was investigated by SEM, as shown in Fig. 3((a) and (b)). The results indicate that the sample formed stone morphology of varying size and shape, with a particle size of 3–10 μm, approximately. High-resolution SEM analysis indicates that the sample is nonporous (not shown here). This is in accordance with the result of BET surface area presented in Table 2. From Fig. 3(b), the surface of the LDH sample becomes rough after sorption of phosphate, indicating some interactions between the LDH sample and solution, due to the uptake of phosphate ions by anion-exchange and electrostatic attraction.

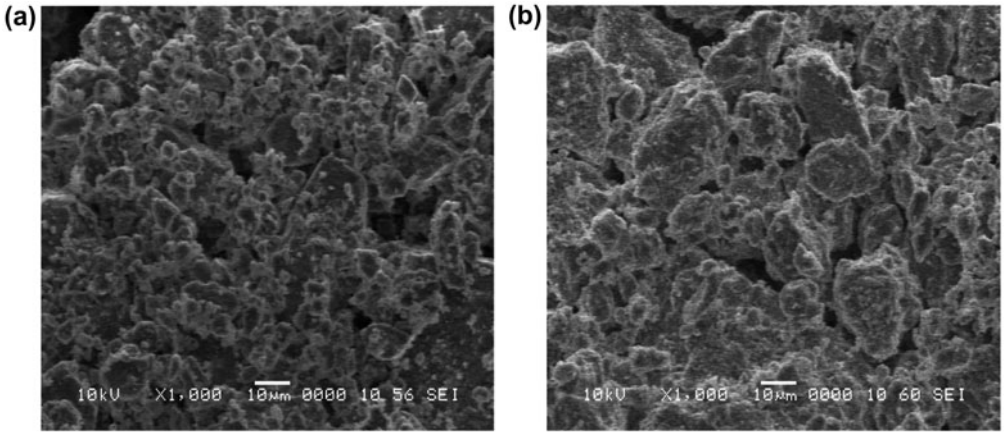

Fig. 3. SEM images of MgAl-NO_3 LDH: (a) before and (b) after sorption of phosphate.

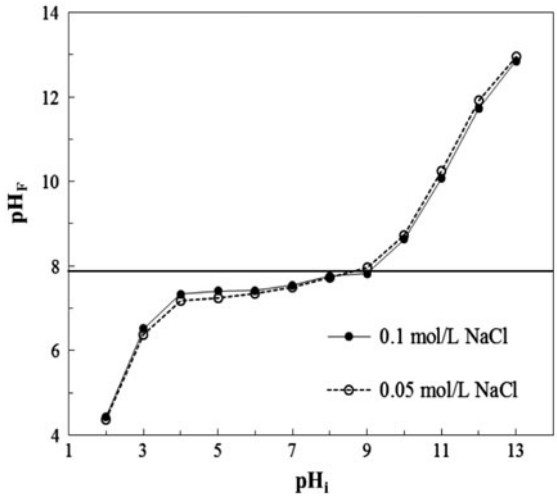

Fig. 4. pH_{final} as a function of $pH_{initial}$ for MgAl-NO_3 LDH: (T = 20℃, m = 0.05 g, V_{NaCl} = 250 mL, Ø = 50–100 μm).

The pH_{zpc} of MgAl-NO_3 LDH is around 7.8 as revealed by crossing point of the curves (Fig. 4), indicating an amphoteric surface, which is positively charged at pH lower than 7.8, while negatively charged when pH is higher than 7.8. Therefore, in addition to the main ion-exchange mechanism, there is electrostatic attraction between negative phosphate species ($H_2PO_4^-$ and HPO_4^{2-}) and electropositive LDH surface since the solution pH was below the pH_{zpc} of material.

3.2. Sorption properties

3.2.1. Effect of pH

The pH of solution is an important parameter that influences the sorption of anions at the solid–liquid interface [42]. The effect of solution pH on phosphate removal by MgAl-NO_3 LDH is shown in Fig. 5.

Fig. 5 shows that phosphate removal onto MgAl-NO_3 LDH is pH dependent. It appears that the sorption capacity decreased slightly at much lower pH of 2 and the phosphate removal was about 90%. This may be due to slow dissolution of LDH at too lower pH.

However, at pH ranging from 3 to 7, phosphate removal remains almost constant and phosphate ions are practically entirely removed. Inside this pH range, $H_2PO_4^-$ is the dominant species of phosphate [43]. Anion-exchange easily occurred between $H_2PO_4^-$ ions and the interlayer nitrate, resulting in a high uptake of phosphate. When the pH of solution is lower than pH_{zpc}, the surface of LDH is positively charged. The electrostatic attraction between the negatively charged surface and electronegative phosphate species contributes in the removal process. Therefore, phosphate ions were removed by a combination of both electrostatic attraction and anion-exchange mechanisms.

At a pH value of 8 ($pH > pH_{zpc}$), the removal efficiency does not change. The surface of LDH is negatively charged and $H_2PO_4^{2-}$ ions became the dominant species. The electrostatic attraction does not occur and anion-exchange is the main mechanism in the sorption process.

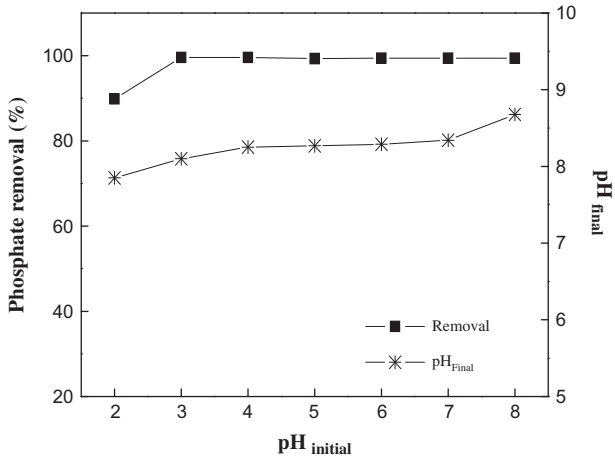

Fig. 5. Effect of initial pH on phosphate sorption by MgAl-NO_3 LDH: (C_0 = 100 mg/L, m = 2 g/L, T = 20℃, W = 200 rpm).

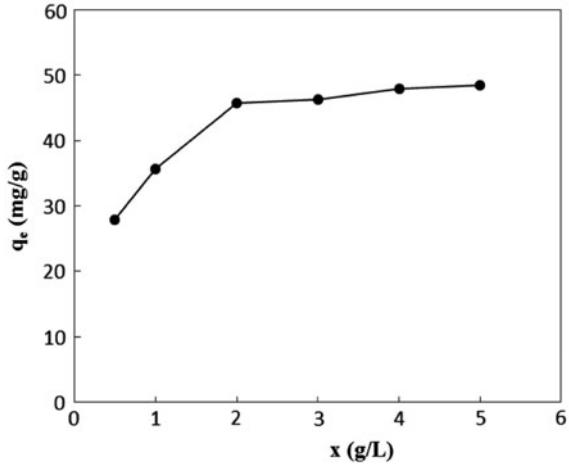

Fig. 6. Effect of sorbent dosage on phosphate sorption by MgAl-NO_3 LDH: (pH 6, C_0 = 100 mg/L, T = 20℃, W = 200 rpm).

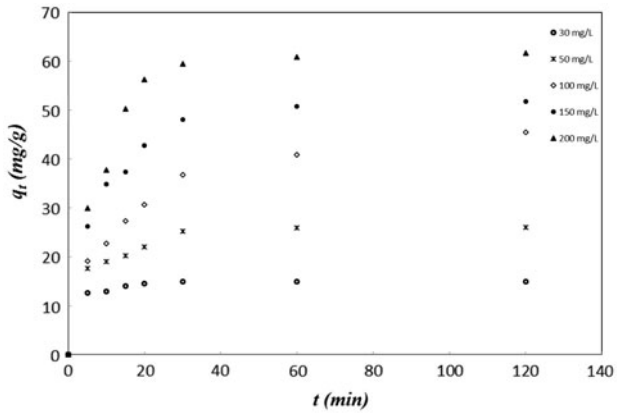

Fig. 7. Effect of initial concentration on phosphate sorption by MgAl-NO_3 LDH: (pH 6, $m = 2$ g/L, $T = 20$°C, $W = 200$ rpm).

At equilibrium, the pH of solution increased, offering pH values between 8 and 9, due to the release of hydroxide ions from the layers of LDH material.

In the wastewater treatment plant, the pH of wastewater is adjusted to 7 before discharging into water bodies. At this pH value, the removal of phosphate by MgAl-NO_3 LDH is more than 95%. Therefore, in view of practical application, adjusting the pH of wastewater is not needed.

3.2.2. Effect of sorbent dosage

The effect of sorbent dosage on phosphate removal is shown in Fig. 6.

The results show that the sorption capacity increases rapidly from 27.62 to 46.57 mg/g with increasing the sorbent dose from 0.5 to 2 g/L, respectively. This is due to the availability of the exchangeable sites for phosphate sorption at higher sorbent dose. However, phosphate uptake remains almost constant at 46.57 mg/L with the increase of sorbent dose from 2 to 5 g/L. This suggests the existence of the optimum dose for the maximum phosphate uptake at 2 g/L.

3.2.3. Effect of initial concentration

The effect of initial concentration on phosphate removal is shown in Fig. 7.

Phosphate uptake was rapid in the first step, at the beginning up to 20 min, then slowed considerably till a saturation level was reached at 30 min. The initial rapid phase may be due to greater number of sorption sites available for phosphate uptake. After 30 min, although the phosphate uptake has a slight increase with increasing the contact time, it remains almost constant, meaning that the sorption equilibrium of phosphate is reached.

In order to explain the mechanism involved in sorption process, three kinetic models were applied, such as pseudo-first-order model (Eq. (7)) [44], pseudo-second-order model (Eq. (8)) [45], and intraparticle diffusion model (Eq. (9)) [46].

$$\ln(q_e - q) = \ln q_e - k_1 t \tag{7}$$

$$t/q = 1/\left(k_2 q_e^2\right) + t/q_e \tag{8}$$

$$q = k_i t^{1/2} + C \tag{9}$$

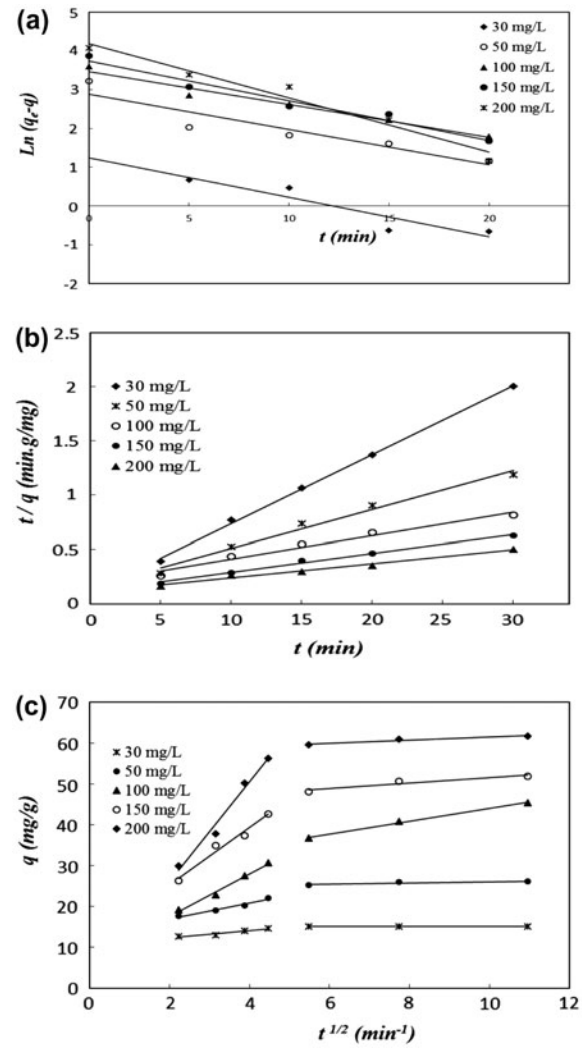

Fig. 8. Kinetic plots regression for phosphate sorption onto MgAl-NO_3 LDH: (a) pseudo-first-order, (b) pseudo-second-order, and (c) intraparticle diffusion models.

where q_e and q (mg/g) are the sorption capacity at equilibrium and time t, respectively. k_1 (min^{-1}) and k_2 (g/(mg min)) are the pseudo-first-order and pseudo-second-order rate constants, k_i (mg/g $min^{0.5}$) is the intraparticle diffusion rate constant, and C is the intercept.

The kinetic parameters are measured from the slope and intercept of the linear plot of model equations, as shown in Fig. 8(a–c).

In compliance with experimental results, calculated q_e increased with increasing initial concentration. At given C_0, q_{e2} values were higher than q_{e1}, which is a general rule. The rate constants varied with C_0. However, variations in k_1, k_2, and k_i values are commonly reported, an increase in k_1 and k_i while a decrease in k_2 with increasing C_0 most frequently ascertained [11,13].

Moreover, calculated parameters are in the range of those reported by others for phosphate removal on diverse in comparable concentrations [47,48].

As shown in Fig. 8(c), the plots of q_t vs. $t^{1/2}$ are not linear within the whole sorption time, showing that the phosphate removal on MgAl-NO_3 LDH does not agree with the intraparticle diffusion model. However, it appears that each plot can be divided into two phases. From Table 3, correlation coefficients of every fitted plot are more than 0.93, indicating that the intraparticle diffusion model gives a good simulation within the corresponding sorption period, implying that the intraparticle diffusion occurs in the uptake process. However, intraparticle diffusion is not the only rate-limiting step because of every phase plot is not passing through the origin, as shown Fig. 8(c) [49,50].

The first sharper region is a gradual sorption stage, due to the anion-exchange reaction between phosphate and interlayer nitrate of LDH. Then, the second region is the equilibrium stage as the uptake of phosphate started to slow down.

Based on the regression coefficients and calculated q_e for each model, the pseudo-first-order and intraparticle diffusion models are not fully valid for the present system. Contrariwise, a good agreement with the pseudo-second-order model was observed at various concentrations, as shown in Fig. 8(b). The correlation coefficients for the linear plot of pseudo-second-order model are more than 0.98 in most cases. Moreover, experimental and calculated q_e show good agreement (Table 3).

Therefore, the removal of phosphate by MgAl-NO_3 LDH is kinetically controlled by a pseudo-second-order reaction rather than a pseudo-first-order process. Hence, chemisorption is the rate-limiting step in sorption process [8,51].

3.3. Equilibrium isotherms

The sorption isotherm of phosphate by MgAl-NO_3 LDH is shown in Fig. 9.

According to the classification of Giles et al. [52], sorption isotherm is H-type, which indicates high affinity between phosphate and LDH sample so that phosphate ions are almost completely sorbed from dilute solution. As shown in Fig. 10(a–c), Langmuir, Freundlich, and Dubinin–Radushkevich models were applied to describe the sorption behavior at equilibrium.

The model parameters are listed in Table 4. From R^2 and q_m values, it appears that the equilibrium data fitted well the Langmuir isotherm (R^2 = 0.999), indicating the monolayer sorption of phosphate onto MgAl-NO_3 LDH. In addition, the R_L value less than unity

Table 3
Sorption parameters of the pseudo-first-order, pseudo-second-order and intraparticle diffusion models at various concentrations

		Initial concentration (mg P/L)				
Kinetic model	Parameter	30	50	100	150	200
Pseudo-first-order	K_1 (min^{-1})	0.101	0.091	0.095	0.102	0.140
	q_{e1} (mg/g)	10.16	17.92	32.19	41.91	55.99
	$q_{e,exp}$ (mg/g)	14.97	25.30	36.71	48.06	59.51
	R^2	0.865	0.869	0.961	0.968	0.965
Pseudo-second-order	K_2 (g/mg min)	0.039	0.008	0.005	0.003	0.002
	q_{e2} (mg/g)	15.75	26.01	36.08	51.80	65.13
	$q_{e,exp}$ (mg/g)	14.97	25.30	36.71	48.06	59.51
	R^2	0.999	0.984	0.980	0.991	0.985
Intraparticle diffusion	k_i (mg/g $min^{0.5}$)	0.78	2.35	5.47	6.59	9.83
	C (mg/g)	10.83	11.82	6.31	12.53	8.95
	R^2	0.941	0.967	0.978	0.983	0.938

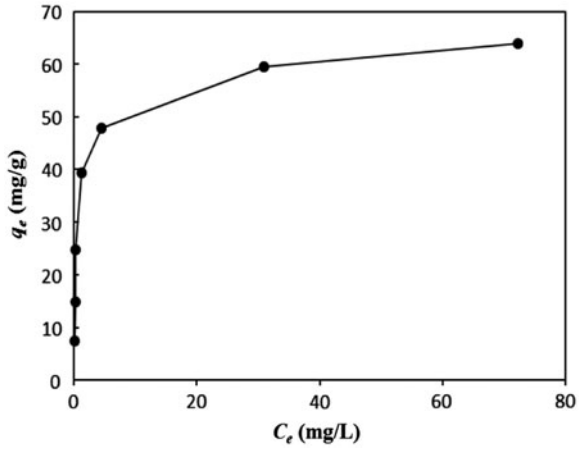

Fig. 9. Sorption isotherm of phosphate by MgAl-NO_3 LDH: (pH 6, m = 2 g/L, T = 20℃, W = 200 rpm).

indicates favorable sorption of phosphate on this sorbent.

Freundlich and D–R isotherms are not as adequate as Langmuir model. The calculated q_m using Langmuir model is close to that obtained at equilibrium (Table 4), while the D–R isotherms give a maximum capacity not compatible with experimental q_m. For Freundlich model, $1/n$ value was between 0 and 1, indicates favorable sorption of phosphate at the studied conditions. As reported by Mckay et al. [53], the n value situated between 2 and 10 represents a good sorption.

The D–R isotherm model determines also the nature of sorption processes. The E (kJ/mol) value gives information about sorption mechanism (physical or chemical). It has been reported that the sorption energy is less than 20 kJ/mol for an anion-exchange controlled process [54]. The calculated sorption energy of 14.87 kJ/mol indicates that the anion-exchange is the determining mechanism for phosphate removal. The anion-exchange process has also been confirmed by XRD pattern and FTIR spectra of LDH sample.

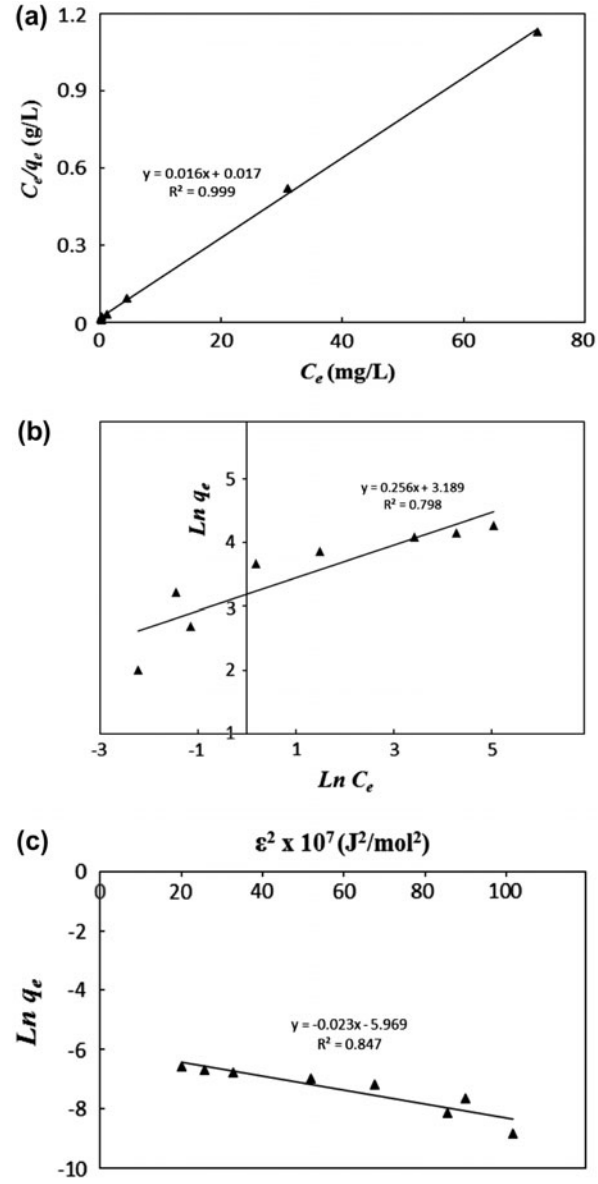

Fig. 10. Langmuir (a), Freundlich (b), and Dubinin–Radushkevich (c) plots for phosphate sorption onto MgAl-NO_3 LDH.

3.4. Regeneration and reusability tests

Once the sorption process is completed, desorption of phosphate from LDH sample is essential to regenerate the sorbent. From the point of view of process overall economy for wastewater treatment by sorption, sorbent reusability is of crucial importance. In order to evaluate the regeneration ability, phosphate sorbed LDH was calcined at 500℃ to displace entirely the interlayer region. Then, the calcined LDH was dispersed into $NaNO_3$ solution at 0.5 M to reconstruct the LDH structure using memory effect. This phenomenon is one of their most attractive features as adsorbents for anionic species [55]. The reusability of LDH sample was assessed for four sorption–regeneration cycles whose results are given in Fig. 11. The results show a slight decrease in sorption capacity with cycles, which attains 28 mg/g in the fourth cycle for treatment of wastewater containing 100 mg P/L. This is due to slight damage in the original LDH structure with regeneration of LDH sample.

Fig. 12((a) and (b)) shows the XRD patterns of phosphate sorbed LDH after calcination and

Table 4
Isotherm model parameters for phosphate sorption onto MgAl-NO_3 LDH

Isotherm model	Parameter	Value	R^2
Langmuir	K (L/mg)	0.94	
	q_m (mg/g)	64.10	0.999
	R_L	0.004	
Freundlich	N	3.91	
	$1/n$	0.25	0.798
	K_F (mg/g)	24.27	
Dubinin–Radushkevich	K_{DR} (mol^2/J^2)	2.35×10^{-9}	
	q_m (mg/g)	132.97	0.847
	$E = (2K_{DR})^{-0.5}$ (kJ/mol)	14.87	

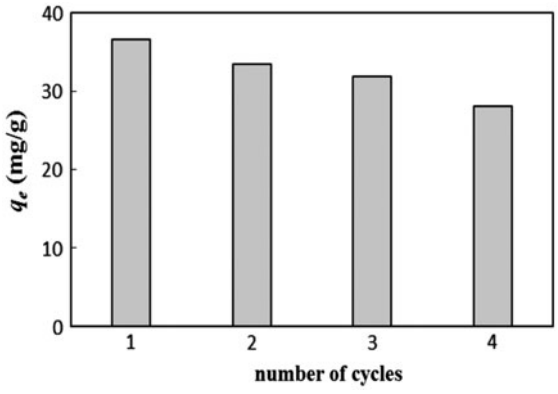

Fig. 11. Evolution of sorption capacity over four consecutive sorption–regeneration cycles: (C_0 = 100 mg/L, m = 2 g/L, T = 20°C, W = 200 rpm).

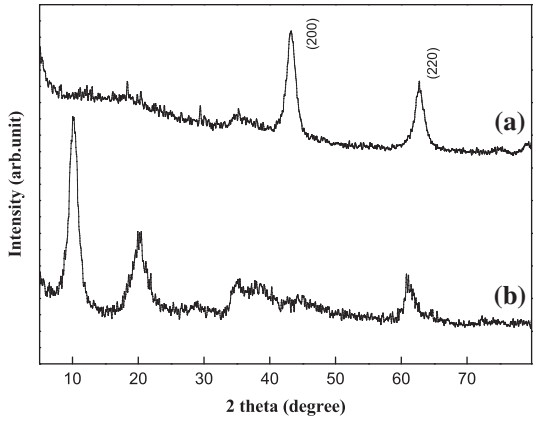

Fig. 12. XRD patterns of phosphate sorbed MgAl-NO_3 LDH: (a) after calcination at 500°C and (b) rehydratation in $NaNO_3$ solution 0.5 M.

rehydratation in $NaNO_3$ solution 0.5 M. After calcination, it appears that the characteristic peaks of LDH structure disappeared and two new broad peaks were observed at high 2θ angles of 43.5° and 63°, corresponding to the (2 0 0) and (2 2 0) reflections, respectively [56]. This indicates that the layered structure of material was destroyed and transformed into amorphous phase when heated at 500°C, due to the decomposition of LDH sample into mixed oxides of Mg and Al during the thermal treatment.

After reconstruction, the layered structure of calcined LDH was reconstructed, as shown in Fig. 12(b). However, the regenerated sample shows low crystallinity compared to its original structure, due to some changes in the LDH structure with calcination.

4. Conclusion

The present investigation evaluated the phosphate removal performance from wastewater using synthesized MgAl-NO_3 LDH as a sorbent material. The structure of material before and after sorption of phosphate was well characterized by XRD and FTIR analysis. It was found that the phosphate removal on MgAl-NO_3 LDH depends on the sorbent dosage, contact time, and initial concentration. MgAl-NO_3 LDH can be used as an efficient sorbent to remove phosphate from wastewater with a good selectivity. The uptake was rapid and reached equilibrium within 30 min. No significant influence of solution pH on phosphate removal was observed at pH ranging from 3 to 8. In addition, sorption kinetic follows pseudo-second-order model, indicating chemisorption of phosphate on this material. The equilibrium data fitted well the Langmuir isotherm, which indicates the monolayer sorption of phosphate onto MgAl-NO_3 LDH. D–R isotherm confirms that anion-exchange is

the controlling mechanism of the overall sorption process. Moreover, Freundlich isotherm reveals that the removal of phosphate is favorable at the studied conditions. The phosphate sorbed LDH can be regenerated in $NaNO_3$ solution and reused in subsequent sorption experiments, with a slight decrease in the sorption capacity.

Nomenclature

C_0	—	initial phosphate concentration (mg/L)
C_t	—	phosphate concentration at time t (mg/L)
C_e	—	phosphate concentration at equilibrium (mg/L)
E	—	sorption energy (J/mol)
K	—	Langmuir constant (L/mg)
K_F and n	—	Freundlich parameters
K_{DR}	—	activity coefficient (mol^2/J^2)
m	—	mass of sorbent (g)
q_t	—	phosphate amount sorbed per gram of sorbent at time t (mg/g)
q_e	—	phosphate amount sorbed per gram of sorbent at equilibrium (mg/g)
q_m	—	saturated sorption capacity of phosphate (mg/g)
R	—	universal gas constant (8.314 J/mol K)
R_L	—	dimensionless equilibrium parameter
T	—	temperature (K)
V	—	volume of solution (L)
W	—	shaking speed (rpm)
x	—	sorbent dose (g/L)
ε	—	Polanyi potential
Ø	—	diameter of sorbent particles (μm)

References

[1] A. Ugurlu, B. Salman, Phosphorus removal by fly ash, Environ. Int. 24(8) (1998) 911–918.

[2] S. Yeoman, T. Stephenson, J.N. Lester, R. Perry, The removal of phosphorus during wastewater treatment: A review, Environ. Pollut. 49 (1988) 183–233.

[3] J. Dai, H. Yang, H. Yan, Y. Shangguan, Q. Zheng, R. Cheng, Phosphate adsorption from aqueous solutions by disused adsorbents: Chitosan hydrogel beads after the removal of copper(II), Chem. Eng. J. 166 (2011) 970–977.

[4] M.W. Kamiyango, W.R.L. Masamba, S.M.I. Sajidu, E. Fabiano, Phosphate removal from aqueous solutions using kaolinite obtained from Linthipe, Malawi, Phys. Chem. Earth 34 (2009) 850–856.

[5] G.K. Morse, S.W. Brett, J.A. Guy, J.N. Lester, Review: Phosphorus removal and recovery technologies, Sci. Total Environ. 212 (1998) 69–81.

[6] Y. Zhao, B. Xi, Y. Li, M. Wang, Z. Zhu, X. Xia, Removal of phosphate from wastewater by using open gradient superconducting magnetic separation as pretreatment for high gradient superconducting magnetic separation, Sep. Purif. Technol. 86 (2012) 255–261.

[7] M. Özacar, Adsorption of phosphate from aqueous solution onto alunite, Chemosphere 51 (2003) 321–327.

[8] Y. Yan, X. Sun, F. Ma, J. Li, J. Shen, W. Han, X. Liu, L. Wang, Removal of phosphate from etching wastewater by calcined alkaline residue: Batch and column studies, J. Taiwan. Inst. Chem. Eng. 45 (2014) 1709–1716.

[9] S. Moharami, M. Jalali, Removal of phosphorus from aqueous solution by Iranian natural adsorbents, Chem. Eng. J. 223 (2013) 328–339.

[10] L. Zeng, X. Li, J. Liu, Adsorptive removal of phosphate from aqueous solutions using iron oxide tailings, Water Res. 38 (2004) 1318–1326.

[11] L. Ding, C. Wu, H. Deng, X. Zhang, Adsorptive characteristics of phosphate from aqueous solutions by MIEX resin, J. Colloid Interface Sci. 376 (2012) 224–232.

[12] M.W. Kamiyango, W.R.L. Masamba, S.M.I. Sajidu, E. Fabiano, Phosphate removal from aqueous solutions using kaolinite obtained from Linthipe, Malawi, Phys. Chem. Earth 34 (2009) 850–856.

[13] M. Rathod, K. Mody, S. Basha, Efficient removal of phosphate from aqueous solutions by red seaweed, *Kappaphycus alverezii*, J. Cleaner Prod. 84 (2014) 484–493.

[14] K.H. Goh, T.T. Lim, Z.L. Dong, Application of layered double hydroxides for removal of oxyanions: A review, Water Res. 42 (2008) 1343–1368.

[15] A. Ookubo, K. Ooi, H. Hayashi, Preparation and phosphate ion-exchange properties of a hydrotalcite-like compound, Langmuir 9 (1993) 1418–1422.

[16] K. Xing, H.Z. Wang, L.G. Guo, W.D. Song, Z.P. Zhao, Adsorption of tripolyphosphate from aqueous solution by Mg–Al–CO_3-layered double hydroxides, Colloids Surf., A 328 (2008) 15–20.

[17] S.L. Wang, C.H. Liu, M.K. Wang, Y.H. Chuang, P.N. Chiang, Arsenate adsorption by Mg/Al–NO_3 layered double hydroxides with varying the Mg/Al ratio, Appl. Clay Sci. 43 (2009) 79–85.

[18] K. Yang, L. Yan, Y. Yang, S. Yu, R. Shan, H. Yu, B. Zhu, B. Du, Adsorptive removal of phosphate by Mg–Al and Zn–Al layered double hydroxides: Kinetics, isotherms and mechanisms, Sep. Purif. Technol. 124 (2014) 36–42.

[19] P. Koilraj, S. Kannan, Aqueous fluoride removal using ZnCr layered double hydroxides and their polymeric composites: Batch and column studies, Chem. Eng. J. 234 (2013) 406–415.

[20] T. Hongo, H. Wakasa, A. Yamazaki, Synthesis and adsorption properties of nanosized Mg-Al layered double hydroxides with Cl^-, NO_3^- or SO_4^{2-} as interlayer anion, Mater. Sci. Poland 29 (2011) 86–91.

[21] S. Miyata, Anion-exchange properties of hydrotalcite-like compounds, Clays Clay Miner. 31 (1983) 305.

[22] P.K. Dutta, M. Puri, Anion exchange in lithium aluminate hydroxides, J. Phys. Chem. 93 (1989) 376.

[23] X. Sun, T. Imai, M. Sekine, T. Higuchi, K. Yamamoto, A. Kanno, S. Nakazono, Adsorption of phosphate using calcined Mg_3-Fe layered double hydroxides in a fixed-bed column study, J. Ind. Eng. Chem. 20 (2014) 3623–3630.

[24] R. Chitrakar, S. Tezuka, A. Sonoda, K. Sakane, K. Ooi, T. Hirotsu, Adsorption of phosphate from seawater on calcined MgMn-layered double hydroxides, J. Colloid Interface Sci. 290 (2005) 45–51.

[25] X. Cheng, X.R. Huang, X.Z. Wang, B.Q. Zhao, A.Y. Chen, D.Z. Sun, Phosphate adsorption from sewage sludge filtrate using zinc–aluminum layered double hydroxides, J. Hazard. Mater. 169 (2009) 958–964.
[26] J.Q.S.M. Jiang Ashekuzaman, Preparation and evaluation of layered double hydroxides (LDHs) for phosphate removal, Desalin. Water Treat. (2014) 1–8, doi: 10.1080/19443994.2014.934734.
[27] C. Novillo, D. Guaya, A. Allen-Perkins Avendaño, C. Armijos, J.L. Cortina, I. Cota, Evaluation of phosphate removal capacity of Mg/Al layered double hydroxides from aqueous solutions, Fuel 138 (2014) 72–79.
[28] L. Lv, P. Sun, Z. Gu, H. Du, X. Pang, X. Tao, R. Xu, L. Xu, Removal of chloride ion from aqueous solution by ZnAl-NO_3 layered double hydroxides as anion-exchanger, J. Hazard. Mater. 161 (2009) 1444–1449.
[29] L.Y. Tian, W. Ma, M. Han, Adsorption behavior of Li^+ onto nano-lithium ion sieve from hybrid magnesium/lithium manganese oxide, Chem. Eng. J. 156 (2010) 134–140.
[30] APHA, Standard methods for the examination of water and wastewater, twenty first ed., American Public Health Association, Washington, DC, 2005.
[31] I. Langmuir, The adsorption of gases on plane surfaces of glass, mica and platinum, J. Am. Chem. Soc. 40 (1918) 1361–1403.
[32] K. Kadirvelu, C. Namasivayam, Agricultural by-products as metal adsorbents: sorption of lead(II) from aqueous solutions onto coir-pith carbon, J. Membr. Sci. 165 (2000) 159–167.
[33] A. Tassist, H. Lounici, N. Abdi, N. Mameri, Equilibrium, kinetic and thermodynamic studies on aluminum biosorption by a mycelial biomass (*Streptomyces rimosus*), J. Hazard. Mater. 183 (2010) 35–43.
[34] T. Lv, W. Ma, G. Xin, R. Wang, J. Xu, D. Liu, Fujun Liu, Physicochemical characterization and sorption behavior of Mg–Ca–Al (NO_3) hydrotalcite-like compounds toward removal of fluoride from protein solutions, J. Hazard. Mater. 237–238 (2012) 121–132.
[35] V. Srinivasa, P. Prasanna, K. Vishnu, Chromate uptake characteristcs of the pristine layred double hydroxides of Mg with Al, Solid State Sci. 10 (2008) 260–266.
[36] Q. Wang, Z. Wu, H.H. Tay, L. Chen, Y. Liu, J. Chang, Z. Zhong, J. Luo, A. Borgna, High temperature adsorption of CO_2 on Mg-Al hydrotalcite: Effect of the charge compensating anions and the synthesis pH, Catal. Today 164 (2011) 198–203.
[37] V. Rives-arnau, G. Munuera, J.M. Criado, Raman spectrum of the split ν_4 mode of $CO^{[dbnd]}{}_3$ ions in aragonite, Spectrosc. Lett. 12 (1979) 733–738.
[38] F.M. Labajos, V. Rives, M.A. Ulibarri, Effect of hydrothermal and thermal treatments on the physicochemical properties of Mg-Al hydrotalcite-like materials, J. Mater. Sci. 27 (1992) 1546–1552.
[39] H. Zaghouane-Boudiaf, M. Boutahala, C. Tiar, L. Arab, F. Garin, Treatment of 2,4,5-trichlorophenol by MgAl–SDBS organo-layered double hydroxides: Kinetic and equilibrium studies, Chem. Eng. J. 173 (2011) 36–41.
[40] F. Cavani, F. Trifirò, A. Vaccari, Hydrotalcite-type anionic clays: Preparation, properties and applications, Catal. Today 11 (1991) 173–301.
[41] H.L. Liu, X.F. Sun, C.Q. Yin, C. Hu, Removal of phosphate by mesoporous ZrO_2, J. Hazard. Mater. 151 (2008) 616–622.
[42] K. Barthélémy, S. Naille, C. Despas, C. Ruby, M. Mallet, Carbonated ferric green rust as a new material for efficient phosphate removal, J. Colloid Interface Sci. 384 (2012) 121–127.
[43] D.W. Oxtoby, H.P. Gillis, A. Campion, H.H. Helal, K.P. Gaither, Principles of Modern Chemistry, seventh ed., Cengage Learning, Washington, 1998.
[44] D. Enshirah, N. De Silva, A. Sayari, Adsorption of copper on amine functionalized SBA-15 prepared by co-condensation: Kinetic properties, Chem. Eng. J. 166 (2011) 454–459.
[45] E. Demirbas, N. Dizge, M.T. Sulak, M. Kobya, Adsorption kinetics and equilibrium of copper from aqueous solutions using hazelnut shell activated carbon, Chem. Eng. J. 148 (2009) 480.
[46] J.W. Weber, J.C. Morris, Kinetics of adsorption on carbon from solution, J. Sanit. Eng. Div. Am. Soc. Civ. Eng. 89 (1963) 31–60.
[47] Y. Yan, X. Sun, F. Ma, J. Li, J. Shen, W. Han, X. Liu, L. Wang, Removal of phosphate from wastewater using alkaline residue, J. Environ. Sci. China 26 (2014) 970–980.
[48] X. Cheng, X. Huang, X. Wang, D. Sun, Influence of calcination on the adsorptive removal of phosphate by Zn–Al layered double hydroxides from excess sludge liquor, J. Hazard. Mater. 177 (2010) 516–523.
[49] E. Bulut, M. Özacar, İ.A. Şengil, Equilibrium and kinetic data and process design for adsorption of Congo Red onto bentonite, J. Hazard. Mater. 154 (2008) 613–622.
[50] X.J. Hu, J.S. Wang, Y.G. Liu, X. Li, G.M. Zeng, Z.L. Bao, X.X. Zeng, A.W. Chen, F. Long, Adsorption of chromium (VI) by ethylenediamine-modified cross-linked magnetic chitosan resin: Isotherms, kinetics and thermodynamics, J. Hazard. Mater. 185 (2011) 306–314.
[51] P. Senthil Kumar, C. Vincent, K. Kirthika, K. Sathish Kumar, Kinetics and equilibrium studies of pb^{2+} ion removal from aqueous solutions by use of nano-silver-sol-coated activated carbon, Braz. J. Chem. Eng. 27 (2010) 339–346.
[52] C.H. Giles, T.H. MacEwan, S.N. Nakhwa, D. Smith, 786. Studies in adsorption. Part XI. A system of classification of solution adsorption isotherms, and its use in diagnosis of adsorption mechanisms and in measurement of specific surface areas of solids, J. Chem. Soc. 786 (1960) 3973–3993.
[53] G. McKay, H.S. Blair, J.K. Gardner, Adsorption of dyes on chitin. I. Equilibrium studies, J. Appl. Polym. Sci. 27 (1982) 3043–3057.
[54] Y.S. Ho, J.C.Y. Ng, G. McKay, Kinetics of pollutant sorption by biosorbents: Review, Sep. Purif. Rev. 29 (2000) 189–232.
[55] K. Chibwe, W. Jones, Intercalation of organic and inorganic anions into layered double hydroxides, J. Chem. Soc. Chem. Commun. 14 (1989) 926–929.
[56] A. Bakhti, M.S. Ouali, Sorption of chromate ions on a calcined synthetic hydrotalcite, Water Qual. Res. J. Can. 40 (2005) 177–183.